Spatio-temporal patterns of whiting (*Merlangius merlangus*) in the Adriatic Sea under environmental forcing

Emanuele Asciutto[1,2¶], Federico Maioli[1¶*], Chiara Manfredi[1,3], Alessandra Anibaldi[1,3], Jacopo Cimini[1], Igor Isailović[4], Bojan Marčeta[5], Michele Casini[1,3,6 *]

[1] University of Bologna, Department of Biological, Geological and Environmental Sciences, Laboratory of Marine Biology and Fisheries, Viale Adriatico 1/n, 61032 Fano, Italy

[2] Department of Integrative Marine Ecology (EMI), Stazione Zoologica Anton Dohrn, National Institute of Biology, Ecology and Marine Biotechnology, Sicily Marine Centre, c/o Villa Pace, Contrada Porticatello 29, 98167 Messina, Italy

[3] CoNISMa, Piazzale Flaminio 9, 00196 Rome, Italy

[4] Institute of Oceanography and Fisheries, Šetalište Ivana Meštrovića 63, 21000 Split, Croatia

[5] Fisheries Research Institute of Slovenia, Spodnje Gameljne 61a, 1211 Ljubljana- Šmartno, Slovenia

[6] Swedish University of Agricultural Sciences, Department of Aquatic Resources, Institute of Marine Research, 45330 Lysekil, Sweden

*** Corresponding authors:**
f.maioli@unibo.it; michele.casini@slu.se; m.casini@unibo.it

¶These authors have contributed equally to this work and share first authorship

Abstract

Understanding how environmental factors affect species distribution is crucial for the conservation and management of marine organisms, especially in the face of global changes. Whiting (*Merlangius merlangus*) is a demersal temperate fish, considered a 'relict species' in the Adriatic Sea. Despite its significance to commercial fisheries in the region, the specific drivers behind its spatial and temporal patterns have not been thoroughly examined. Here, we fitted a set of Generalized Linear Mixed Effects Models to data collected in the Northern and Central Adriatic from 1999 to 2019 during the Mediterranean International Trawl Survey to investigate the potential influence of depth, seafloor temperature and bottom dissolved oxygen on the annual biomass density and spatial distribution of whiting. Our results showed that

depth, and to a lesser degree temperature and oxygen, are important predictors of whiting distribution in spring-summer, with preferences for depths of ~ 45 m, temperature of ~ 15.4 °C and dissolved oxygen > 5.5 ml L^{-1}. We predicted a persistent core area of distribution in front of the Po River Delta, in the Northern Adriatic Sea, while the density progressively declined towards the Central and Southern Adriatic Sea along the Italian coast. Additionally, the temporal trend exhibited high fluctuations over the years, occurring in cycles of 3 to 4 years. Finally, by comparing the biomass density estimates obtained under optimum conditions with those derived from the actual values for each variable, our analysis revealed that temperature had a pronounced and general impact on biomass density in the northern survey area (prediction revealed a ratio of density reduction of approximatively a half), while oxygen displayed a minor and more localized influence. This work deepens the current knowledge about the ecology of whiting in the Adriatic Sea and provides support for the conservation and management of this species.

1 Introduction

Tracking and understanding the effects of environmental factors on the distribution of marine organisms is crucial for the management of species of conservation or commercial interest [1,2], especially in light of major global changes. As a matter of fact, marine species are quickly reorganizing due to climate change [3], even faster than species on land [4]. Generally, marine species are expected to shift poleward [5,6], but also towards deeper and colder areas where local geographical barriers impede latitudinal shifts [7,8]. However, departures from these expectations might occur because of individual species responses, local and regional factors [9], differences in species interactions and stochastic factors [10,11]. Moreover, organisms are likely exposed to diverse aspects of climate change, e.g. changes in sea water level and

temperature, acidification, deoxygenation, modifications in rivers run-off, and change in frequency and strength of adverse weather conditions [12]. This picture is further complicated by the potential effects of other anthropogenic drivers including eutrophication [13], fishing pressure [14,15], pollution [16], and habitat degradation [10], which may interact with climate change at multiple scales.

The impact of global changes on marine species is particularly severe in areas where range shifts are physically constrained, such as in semi enclosed areas [17]. The Adriatic Sea is a semi-closed basin of the Mediterranean Sea which has experienced significant environmental fluctuations and ecosystem degradation linked to the combined effects of climate change, increasing fishing effort and eutrophication in recent decades [18–21]. The marine species living in this basin seem to be particularly vulnerable to environmental disturbances (e.g., long term temperature change, modification of hydrological regime, changes in production and food availability; [22,23]).

Here, we employed data from two decades of fishery-independent surveys to investigate the effects of environmental drivers on whiting, *Merlangius merlangus,* in the Northern-Central Adriatic Sea where this species constitutes a common species of the demersal community [24]. Whiting is a cold-temperate demersal fish widely distributed in the North-East Atlantic Ocean [25], whereas in the Mediterranean Sea [26] and in the Black Sea [27] it represents a 'relict species' which likely migrated from northern waters during the last glacial period [24,28]. In the Mediterranean Sea whiting is particularly abundant in the Northern-Central Adriatic Sea [29], where it is commonly found near muddy or sandy bottoms down to depths of 100 m [30–32]. Some specimens can also be found along the central and southern Italian coast [33]. This species has a relevant role in the fisheries of several countries, and it is included into the list of species of commercial and conservationist interest in the Mediterranean and Black Sea by the General Fisheries Commission for the Mediterranean (GFCM). According to data collected up

to 2017, this species accounted for 3.2% of the total bottom trawl fishery landings in the Adriatic Sea (on a total of 28,800 tons) [34].

Despite the widespread distribution of whiting and its commercial relevance in the Northern-Central Adriatic Sea, many aspects of the ecology of this species have not been analytically investigated so far in this basin. In the present study we use spatio-temporal species distribution models with the aim of a) characterizing the spatial and temporal variation in whiting biomass and b) investigating the effect of the major environmental factors on its spatio-temporal dynamics.

2 Materials and methods

2.1 Study area

The study area is represented by the Northern-Central Adriatic Sea, a semi-enclosed basin corresponding to the FAO - Geographical Sub-Area (GSA) 17 [35] located in the Central Mediterranean, between the Italian peninsula and the Balkans. The basin is a shallow and mainly eutrophic sea with clear morphological differences along both the longitudinal and the latitudinal axes. Most of the basin is characterized by a wide continental shelf where depth gradually increases from North to South. Sea bottom is mostly covered with recent muddy and coastal sandy sediments supplied by rivers and dispersed by marine current, while the offshore seabed in the Northern Adriatic is characterized by relict sand [36]. The eastern coast is rocky and articulated with many islands whereas the western one is flat, alluvial, and characterized by heavy river runoff. The Po and the other northern Italian rivers contribute to approximately 20% of the whole Mediterranean river runoff [37] and introduce large fluxes of nutrients [38], making this basin the most productive area of the Mediterranean Sea [39] and consequently

one of the most intensively fished areas in Europe [40]. The general pattern of water circulation is cyclonic with water masses inflow from the Eastern Mediterranean along the eastern side of the Adriatic Sea and outflow along the western side. Being a continental basin, the Adriatic Sea circulation and water masses are strongly influenced by river runoff and atmospheric conditions that affect salinity and temperature [41]. Pronounced seasonal fluctuations in environmental forcing, cause high seasonal variation in coastal waters, where bottom temperatures, range from 7 °C in winter to 27 °C in summer [42]; in the deeper areas the thermal variability is reduced, with values ranging between 10 °C in winter and 18 °C in summer at a depth of 50 m [42]. A well-developed thermocline is present in spring and summer [41] which, under suitable marine weather conditions (i.e., high temperatures, extended period of calm sea, freshwater inflow, stratification) can cause exceptional algal blooms and extended hypoxia and anoxia phenomena that damage the demersal and the benthic communities [43].

2.2 Data source

2.2.1 Survey data

Biomass density data of whiting (i.e., estimated as the ratio between the total weight of fish caught and the area swept in each haul, expressed as kg km^{-2}) were obtained from standardized experimental trawl hauls carried out in the GSA 17, within the frames of the Mediterranean International Trawl Survey (MEDITS). This survey started in 1994 at the European Mediterranean level, with the aim to collect data on demersal communities to describe their distribution and demographic structure [44,45]. The MEDITS covers the whole GSA 17 since 1996 and it is jointly performed by the Laboratory of Marine Biology and Fisheries of Fano (Italy), the Institute of Oceanography and Fisheries of Split (Croatia) and the Fishery Research Institute of Slovenia. Between 88 and 247 trawl hauls were performed annually, typically

during the late spring-summer season (May-September) using an experimental bottom trawl with 20 mm of stretched mesh cod-end. Hauls were located from 10 to 500 m of depth, following a random-stratified sampling scheme where strata were defined according to depth. Further details on sampling procedures, data collection and analysis can be found in the MEDITS handbook [46]. In the present study, we included trawl hauls performed between 1999 and 2019 because of the lack of seafloor dissolved oxygen data for earlier years. In order to have a more seasonal-homogeneous dataset, we included only the hauls performed in May-September and removed those conducted in the autumn-winter period (i.e., October-December) (S1 Fig).

2.2.2 Environmental variables

In order to investigate major changes in the environmental covariates and potentially concurrent changes in whiting biomass density, we specifically focused on three key factors: depth, seafloor temperature (hereafter temperature; T), and seafloor dissolved oxygen (hereafter dissolved oxygen; DO). These factors were selected based on previous knowledge [47] and data availability. T and DO data used in this study were obtained from the E.U. Copernicus Marine Service Information [48,49] extracting the monthly mean of each variable. Hence, to integrate the environmental data with the survey data, we associated each survey haul with the nearest spatial point where the variables were available, as well as the nearest corresponding time reference for the haul.

2.3 Statistical analysis

2.3.1 Quantifying local environmental trends

To assess and visualize potential changes in the environmental drivers, we estimated the mean values across the study area and years as well as their local rate of change. To achieve this, we constructed a 2 km^2 grid (UTM 33N projection) encompassing the entire survey area, and matched the environmental covariates as described is section 2.2.2. Additionally, depth data was retrieved from the EMODnet Bathymetry project, https://www.emodnet.eu/en/bathymetry, funded by the European Commission Directorate General for Maritime Affairs and Fisheries. Thereafter, for temperature and dissolved oxygen, we employed a linear model for each grid cell, adopting the following form:

$$Y \sim \text{Normal}(\mu, \sigma^2) \# (7)$$

$$\mu = \alpha + \beta \text{Year} \# (8)$$

Here, Y denotes the environmental covariate value at the cell, μ denotes the mean of the cell, and σ represents the standard deviation. The intercept is denoted by α, and the coefficient related to year is represented by β. The local rate of change can be derived from the β slope. To facilitate interpretation, we presented the local (i.e., the grid cell) rate of change as decadal trends.

2.3.2 Spatio-temporal models

The spatio-temporal distribution of whiting was analysed using geostatistical Generalized Linear Mixed Effects Models (GLMMs) fitted by maximum marginal likelihood using the sdmTMB R package (version 0.0.21.9;[50]) in R (version 4.0.3; [51]). Biomass density was modelled with a Tweedie distribution and a log link function to accommodate both zeros and positive continuous values [52]:

$$y_{s,t} = \text{Tweedie}(\mu_{s,t}, p, \phi), 1 < p < 2 \ \#(1)$$

$$\mu_{s,t} = \exp(\alpha_t + \text{X} + \omega_s) \#(2)$$

$$\alpha_t = \text{N}(0, \sigma_\alpha^2) \#(3)$$

$$\omega_s \sim \text{MVNormal}(0, \Sigma_\omega) \#(4)$$

Where $y_{s,t}$ is the biomass density (kg km^{-2}) at point $\boldsymbol{s}$ in space and t in time, $\boldsymbol{\mu}_{s,t}$ the mean biomass density, p the Tweedie power parameter and ϕ the Tweedie dispersion parameter. The parameter α_t is the random intercept by year t with variance σ_a. The parameter $\boldsymbol{X}$ represents the design matrix of the covariates (which are specified in Table 1). The $\boldsymbol{\omega}_s$ parameter represents a spatial random field. Spatial random fields are assumed to be drawn from a multivariate Gaussian distribution with covariance matrix $\boldsymbol{\Sigma}_\omega$ and constrained by a Matérn covariance function. Following Essington et al., 2022 [53], we intentionally omitted the spatiotemporal random fields (ε_t) to specifically focus on examining the relationship between inter-annual changes in biomass density and variations in T and DO. The inclusion of spatiotemporal random fields introduces an additional complexity when attempting to disentangle the individual effects of T and DO on biomass density changes [53].

Table 1 Models' formulations and model selection results. Df are the degrees of freedom. DoY is the day of the year, T is the temperature and DO is the dissolved oxygen. AIC represent the scores of the Akaike Information Criterion.

Model	Formula	df	AIC	ΔAIC
Model 0	Depth + Depth^2 + DoY + DoY^2	10	13603.43	196.56
Model 1	Depth + Depth^2 + DoY + DoY^2 +T	11	13516.90	110.03
Model 2	Depth + Depth^2 + DoY + DoY^2 + T + T^2	12	13418.62	11.75
Model 3	Depth + Depth^2 + DoY + DoY^2 + DO	12	13518.85	111.98
Model 4	Depth + Depth^2 + DoY + DoY^2 + T + DO	13	13467.52	60.65
Model 5	Depth + Depth^2 + DoY + DoY^2 + T + T^2 + DO	14	13406.87	0.00

2.3.3 Model specification and model selection

All models in our analysis accounted for fixed effects of day of year (DoY) and depth, modelled as linear plus quadratic terms. Models 1 to 5 further incorporated different combinations or specifications of T and DO as covariates (see Table 1). DO was included as a breakpoint (BP) effect, which assumes that there is no effect of DO on biomass density above a certain threshold, while below this threshold, the effect is linear [53]. All covariates were centered and scaled by their standard deviations to aid convergence and facilitate comparison of coefficients [54]. We used the Akaike Information Criterion (AIC, [55]) to compare the performance of the five models with different combinations of covariates.

2.3.4 Spatio-temporal predictions of biomass density

To evaluate changes in whiting biomass density over space and time, we utilized the best-fitting model to predict onto the 2 km^2 grid. We measured the standard errors associated to each grid cell prediction by sampling 500 simulations from the joint precision matrix. By multiplying the area with the biomass density and summing up the results across the entire study region, we derived an overall model-based temporal index of the biomass density for the Northern-Central Adriatic Sea. This index represents the predicted biomass density per year and was further normalized using the first year of the data used (i.e., 1999).

3 Results

3.1 Summary of environmental variables

The northern part of the Adriatic basin is characterized by shallow waters (mean depth of ~ 40 m) with a weak bathymetric gradient along the longitudinal axis (Fig 1a-b). The central area is characterized by meso-Adriatic depressions (Pomo Pits), where the depth decreases to ~ 270 m. In the Northern-Central Adriatic, high seafloor summer temperatures (T) were registered in the Italian shallow coastal areas (~ 25°C), while colder waters were in deeper zones and along the Croatian coast (~ 15°C) (Fig 1c). Over the study period, T increased by an average of ~ 0.30 °C per decade across the entire basin, but with more pronounced warming offshore the Po River Delta, south of the Pomo Pits and along the central and southern Italian coast (up to ~ 1 °C per decade). In contrast, the Gulf of Venice and the central Croatian coast showed a decrease in T of as high as ~ 0.5 °C per decade (Fig 1d). The bottom dissolved oxygen (DO) was lower along the central-southern Adriatic (~ 5.4 ml/L^{-1}) (Fig 1e). The highest values were registered north and south of the Po River Delta and in the Croatian channels (~ 6.0 ml/L^{-1}). DO displayed,

along the study period and across the study area, a decrease by an average of 0.02 ml/L^{-1} per decade, with a general increase in the Northern Adriatic (i.e., areas below Po River Delta, ~ 0.15 ml/L^{-1}) and a slight decrease in the south-western areas (~ -0.05 ml/L^{-1}). A decline in DO was also observed in small areas just below the Istrian Peninsula and along the shore of the Gulf of Venice.

Fig 1. **Study area (a), depth (b), mean temperature (c) and mean dissolved oxygen (d) conditions (June-August) between 1999-2019, and predicted decadal local trends for temperature (d) and oxygen (f).** The local rate of change was calculated for each grid cell (2 km^2).

3.2 Best fitting model and effects of environmental variables

Among the models we tested (listed in Table 1), Model 5 achieved the lowest AIC score, indicating it as the best-fitting model. Model 5 included T, T^2 and DO, in combination with DoY, DoY^2, depth, depth^2, spatial random effects (ω_s), as well as a random year intercept (α_t). The estimated coefficients for Model 5 showed a strong effect of depth, and to a lesser extent of DO and T, even after accounting for spatial random effects (S2 Fig). Despite the presence of some spatial clustering, the residual diagnostics of our model looked satisfactory, indicating that the model adequately captured the relationship between the environmental factors and the distribution of whiting populations. More information about model diagnostics can be found in the Supporting Information (S3 and S4 Figs). We calculated optimal values for each environmental variable and examined the biomass density variation associated with these values. Taking into account the minimum and maximum recorded values for T (9 °C and 28 °C, respectively), the minimum recorded value for DO (4.7 ml L^{-1}), and the shallowest depth considered in the MEDITS protocol (10 m), we evaluated the lower and higher ranges for each

variable (i.e., the variation in biomass density from the minimum and maximum value to the optimum). Based on our analysis, an optimal depth of approximately 45 m (Fig 2a) was estimated for whiting. The mean biomass density exhibited an increase of 1.8 times from shallow depths of 10 m towards the estimated optimum. However, it dropped close to zero at depths exceeding 110 m (Fig 2a). The predicted mean biomass density peaked at an intermediate T of 15.4 °C (Fig 2b). The biomass density displayed an increase of 2.4 times from the cold T of 9 °C to the optimum, while it showed a decrease of -1.9 times from the optimum to highest T of 28 °C. Additionally, we estimated a DO threshold of approximately 5.5 ml L^{-1} (Fig 2c) with a 95% confidence interval of [5.41, 5.62]. Under suboptimal conditions of 4.7 ml L^{-1}, there was a variation in biomass density of - 3.1 times.

Fig 2. **Marginal effects of depth (a), temperature, T (b) and dissolved oxygen, DO (c).** Gray lines represent random draws from the joint precision matrix (with n of simulations = 100) while black lines represent mean values. Depth and T were modelled as a quadratic function to allow for intermediate optima, while DO was modelled as breakpoint function. The red dashed line marks the optima of depth and T, and the breakpoint of DO.

3.3 Spatial and temporal variations in biomass density

Whiting occupied nearly half of the Northern-Central Adriatic Sea (Fig 3a and S5 Fig). Predicted high densities (up to ~ 600 kg km^2) indicated that most of the whiting inhabits the northern part of the basin, with a core area located between the Po River Delta and the Istrian peninsula. Predicted intermediate values of biomass densities (~ 100-150 kg km^{-2}) resulted to be spread around the core area, in the central part of the basin, and along the Italian coast, while the offshore area in the central part of the basin displayed lower densities (as low as ~ 10 kg km^{-2}). Predicted densities reached nearly 0 in the offshore central and southern part of the basin where the depths exceed 140 m, and along the central and southern Croatian coast. During the

entire time series whiting occupied broadly the same areas. The highest standard error values were estimated in the southern part of the basin (Fig 3b). The spatial biomass density predictions for each year of the time-series are available in the Supporting Information (S5 Fig). The overall temporal biomass density index, based on the best-fitting model, exhibited significant fluctuations during the period under investigation (Fig 3c). These fluctuations manifested as consecutive peaks and valleys occurring approximately every 3-4 years.

Fig 3. **Predicted spatio-temporal changes of whiting biomass density (Kg Km-2) (a) with associated standard error of the mean (b). Relative temporal biomass density index normalized to the first year (c).** All predictions were made over a 2 km^2 prediction grid. For the predictions of all the years see S5 Fig in Supporting Information. In panel (c) the values have been standardized to the initial year of the survey, namely 1999, which is represented by the dashed line. The shades around the mean are 95% confidence intervals.

3.4 Predicted biomass density under different scenarios

To further assess the influence of T and DO on whiting, we conducted separate analyses comparing predicted biomass density under different environmental scenarios. For T, we compared two scenarios: one assuming the estimated optimum T at all sites, and the other incorporating the actual T values (Fig 4). Our analysis revealed significant effects of T, particularly in the northern part of the study area (Fig 4). Here, biomass densities were predicted to be reduced by half compared to the expected levels under optimum T conditions. Similarly, we explored the impact of DO levels on whiting by comparing predicted biomass density under two distinct scenarios. The first scenario assumed that DO at all sites exceeded the estimated threshold, while the second scenario utilized the actual extracted values of DO (Fig 5). Our analysis highlighted localized effects of DO, particularly in the coastal areas south of the Po River Delta, extending to the northern study area and along the western side of the

Istrian Peninsula. In these areas, biomass density was predicted to decrease to approximately one-quarter to half of the expected levels observed at the estimated threshold of DO conditions, depending on the specific location.

Fig 4. Map of the the proportional reduction in whiting biomass density attributed to variations in temperature T. The proportional reduction in whiting biomass density is computed as the ratio of predicted densities at the estimated optimal T compared to the actual T, based on the best fitting model. Only cells that cumulatively reached 90% of the whiting biomass density are displayed. The years are displayed considering an interval of 7 starting from the first. All predictions were made over a 2 km^2 prediction grid.

Fig 5. Map of the the proportional reduction in whiting biomass density attributed to variations in dissolved oxygen, DO. The proportional reduction in whiting biomass density is computed as the ratio of predicted densities at the estimated DO threshold compared to the actual DO, based on the best fitting model. Only cells that cumulatively reached 90% of the whiting biomass are displayed. Only the most representative years were displayed. All predictions were made over a 2 km2 prediction grid.

4 Discussion

Our study provides an important step ahead towards a deeper ecological understanding of the response of a demersal species to major environmental variations. Here, by fitting distribution models to two-decades of fishery-independent survey data we show that depth, and to a lesser extent temperature and dissolved oxygen play a major role in shaping whiting spatio-temporal variations in biomass density over the Central-Northern Adriatic Sea. Here, we also provide a temporal index of the biomass density for the entire study area. This allows to visualize the predicted biomass density trend over the years. Furthermore, we compared the biomass densities predicted at the temperature and dissolved oxygen levels that are optimal for whiting

with the densities observed at the actual values of each variable. By quantifying these disparities, we are able to highlight the magnitude of the impact that deviations from the optimal environmental conditions can have on the distribution and abundance of whiting in the Central-Northern Adriatic Sea.

4.1 Effect of environmental factors

Very little previous information is available on the effect of environmental factors on whiting distribution [56,57]. With regard to the Mediterranean Sea, only Papaconstantinou (1982) [26] analysed the distribution of this species in the Aegean Sea as a function of major environmental factors. In our study, we found whiting to preferably inhabit depths of about 45 m, becoming virtually absent at depths > 110 m. This is in agreement with previous studies in the Adriatic Sea [30,58] and consistent with other findings in other areas, such as in the North Sea [59], Black Sea [60] and the Aegean Sea [26,61].

Papaconstantinou (1982) [26] indicated the temperature range of whiting in the Aegean Sea as between 9.4 °C and 17.5 °C with preferences for temperatures higher than 10 °C. This is close to our estimates revealing an optimal temperature of ~ 14.4 °C. Moreover, our results are in accordance with Svetovidov (1948) [62] who suggested that this species in the Black Sea migrates during winter from the colder areas to the warmer areas to find the optimal temperature range of 5 °C - 16 °C. However, the preferred temperatures of 6 - 10 °C reported for adult individuals in the Black Sea [63] as well as of 7 - 11 °C [64] found in the Fishbase database [65] are not completely in accordance with our results. The reason could be that the dataset included in our study only referred to the spring-summer period when water temperatures are higher. Further, we estimated the threshold of dissolved oxygen concentration at ~ 5.5 ml L^{-1}, below which the dissolved oxygen concentration seems to be suboptimal for whiting. The positive relationship between biomass density and oxygen might suggests a

339 tendency for withing to avoid areas with suboptimal dissolved oxygen. Although a threshold
340 of 1.4 ml L^{-1} (~2 mg L^{-1}) is used in most conventional applications as the level below which
341 hypoxic conditions are met and fish stocks may start to collapse [66], as reported by two meta-
342 analyses [67,68] more realistic sub-lethal threshold can vary by one order-of-magnitude among
343 marine organisms. For example, cod *Gadus morhua*, a close relative of whiting, has an
344 estimated sub-lethal threshold of ~ 7.14 ml L^{-1} [67], even higher than our estimate. However,
345 we recall that our threshold is estimated from in-situ observations and is therefore expected to
346 differ from laboratory-conducted experiments. Eventually, our analysis could not exclude size-
347 specific responses to environmental variables that could potentially explain discrepancies with
348 literature in other areas.

349 4.2 Spatio-temporal dynamics

350 Our study show that whiting is mainly distributed in the northern area of the Adriatic Sea, with
351 the core area located in the shallow waters in front of the Po River Delta. Biomass density
352 declines towards the Central Adriatic Sea, where depth increases. The scarce, yet constant,
353 presence of whiting along the southern Italian coast suggests that the cyclonic pattern of water
354 circulation might carry eggs and pelagic larval stages from the northern spawning locations
355 (also corresponding to the adults distribution area; [33]) towards these southern areas [33,69].
356 In the northern part of the basin, we observed an offshore area, located between the Istrian
357 peninsula and the Italian coasts, with systematically lower densities compared to the nearby
358 areas. This area, called "area degli sporchi" (roughly meaning "dirty area") by fishermen, is
359 characterized by relict sand rich in epifaunal organisms, whereas whiting seems to prefer sand-
360 muddy sediments with scarce biocenosis [31,70]. Indeed, we predicted higher whiting densities
361 within the continental shelf of North and Central Adriatic, mostly covered by fine sediments
362 (muddy sand and sandy mud, [71]). Furthermore, these areas are also characterized by a scarcer

density of hake (*Merluccius merluccius*), which may indicate a possible competition for the resources [24]. Moreover, within the Bristol Channel and the Severn Estuary (UK), growth and local abundance of whiting were positively linked to the presence of two preys, the brown shrimp (*Crangon crangon*) and the sprat (*Sprattus sprattus*) [72], which are also present in the northern and central areas of the Adriatic Sea [73,74]. The persistence of whiting in the same areas across years found in our study may depend also on its low tendency to make long distance movements, although the capability of some adult specimens to do so [69]. Overall, biomass density time-series was characterized by high fluctuations with peaks occurring with a frequency of 3 to 4 years, likely due to the short lifespan of this species and driven by strong recruitment events [60,75]. By comparing the biomass density estimates obtained under optimum environmental conditions with those derived from the actual values, we discovered distinct influences of temperature and dissolved oxygen on different areas within the study region. Firstly, the comparison revealed that the northern extent of the survey was primarily influenced by temperature changes. These temperature variations resulted in lower biomass density estimates, indicating that temperature could potentially act as a limiting factor in this area. The observed decrease in biomass density suggests that whiting populations are less abundant in regions experiencing higher temperatures. This finding highlights the sensitivity of whiting to temperature and suggests that temperature plays a critical role in shaping the distribution patterns of this species. In contrast, more localized areas, particularly those located south of the Po River Delta, extending to the northern part of the survey, and along the western side of the Istrian Peninsula, were affected by sub-optimal oxygen levels. These areas exhibited decreased biomass densities, indicating that whiting populations in these regions are influenced by sub-optimal dissolved oxygen levels. However, the impact of sub-optimal oxygen levels was observed within a more limited geographic extent compared to the broader temperature-related effects observed in the northern region. Overall, our study underscores the complex

interplay between depth, temperature, dissolved oxygen, on the spatio-temporal dynamics of whiting, providing crucial insights into the ecological factors shaping the distribution and abundance of this demersal species in the Central-Northern Adriatic Sea.

5 Conclusions

Understanding how environmental factors drive the patterns of species distribution is a key ecological question and a requirement for effective management when fish species are of commercial or conservation interest. Here, we employed species distribution models to provide detailed information on the spatial ecology of whiting in the Central and Northern Adriatic Sea, one of the most commercially trawled areas of the Mediterranean. We showed that depth, and to a minor degree temperature and bottom dissolved oxygen, are important environmental factors in shaping whiting distribution in this basin. We then compared the differences in predicted biomass density between two different scenarios (i.e., optimal conditions and actual values) for temperature and dissolved oxygen. For temperature we found a decline of approximatively a half between the two scenarios, while oxygen displayed a minor and more localized influence. Taking into account the current effects of worldwide climate change, these results could rise awareness for the future status of this species. The effects of climate change might be compounded by the geomorphology of the Adriatic Sea which could act as a "cul-de-sac" preventing whiting from shifting its distribution to higher latitudes [76]. Although dissolved oxygen was recognised as an influent predictor of local whiting biomass density, its temporal changes seemed somehow less related to the local biomass density trends. However, if dissolved oxygen would decline in large areas (e.g. due to climate change, increased river runoff and increased primary production) below the estimated threshold of 5.5 ml L^{-1} it could potentially influence whiting large-scale distribution.

However, the findings of this study must be seen in light of some limitations. Firstly, our analysis did not separate whiting in age nor in length classes but investigated the overall response of the population to environmental variables. Since this response is often stage or length-specific, additional studies should be performed to investigate the potential different effects of environmental variables on different length-classes of whiting. Secondly, climate change may have other effects on whiting than a mere shift in distribution. For instance, organisms can undergo modifications in their reproductive capacities, physiology, phenology, growth, and mortality, leading to changes both at individual and population levels [77]. Whiting remains a not well studied species in the Adriatic Sea. More research is needed to deepen the knowledge of this fish, such as inter- and intra-specific interactions, fishing effects and aspects of its reproduction (e.g., influence of environmental variables on spawning and egg/larvae survival and transport), but also some aspects of its physiology (e.g., tolerance for low oxygen level and for increasing temperatures, and possible coping mechanisms). However, the present study contributes to expanding the actual knowledge on the ecology of whiting in the Adriatic Sea, providing information which might also be used as a baseline for future studies.

Acknowledgments

We would like to warmly thank all the MEDITS team who have contributed to the data collection and organization. We thank Max Lindmark for the critical discussions on the modelling framework.

References

1. Cury PM, Christensen V. Quantitative ecosystem indicators for fisheries management. ICES J Mar Sci. 2005;62: 307–310. doi:10.1016/j.icesjms.2005.02.003

2. Planque B, Loots C, Petitgas P, Lindstrøm U, Vaz S. Understanding what controls the spatial distribution of fish populations using a multi-model approach: Spatial distribution of fish populations. Fish Oceanogr. 2011;20: 1–17. doi:10.1111/j.1365-2419.2010.00546.x

3. Pinsky ML, Fenichel E, Fogarty M, Levin S, McCay B, Martin KS, et al. Fish and fisheries in hot water: What is happening and how do we adapt? 2021;63: 17–26. doi:10.1002/1438-390X.12050

4. Poloczanska ES, Brown CJ, Sydeman WJ, Kiessling W, Schoeman DS, Moore PJ, et al. Global imprint of climate change on marine life. Nat Clim Change. 2013;3: 919–925. doi:10.1038/nclimate1958

5. Parmesan C, Yohe G. A globally coherent fingerprint of climate change impacts across natural systems. Nature. 2003;421: 37–42. doi:10.1038/nature01286

6. Doney SC, Ruckelshaus M, Emmett Duffy J, Barry JP, Chan F, English CA, et al. Climate Change Impacts on Marine Ecosystems. Annu Rev Mar Sci. 2012;4: 11–37. doi:10.1146/annurev-marine-041911-111611

7. Nye J, Link J, Hare J, Overholtz W. Changing spatial distribution of fish stocks in relation to climate and population size on the Northeast United States continental shelf. Mar Ecol Prog Ser. 2009;393: 111–129. doi:10.3354/meps08220

8. Pinsky ML, Selden RL, Kitchel ZJ. Climate-Driven Shifts in Marine Species Ranges: Scaling from Organisms to Communities. Annu Rev Mar Sci. 2020;12: 153–179. doi:10.1146/annurev-marine-010419-010916

9. Pinsky ML, Worm B, Fogarty MJ, Sarmiento JL, Levin SA. Marine Taxa Track Local Climate Velocities. Science. 2013;341: 1239–1242. doi:10.1126/science.1239352

10. Halpern BS, Walbridge S, Selkoe KA, Kappel CV, Micheli F, D'Agrosa C, et al. A Global Map of Human Impact on Marine Ecosystems. Science. 2008;319: 948–952. doi:10.1126/science.1149345

11. Parmesan C, Duarte C, Poloczanska E, Richardson AJ, Singer MC. Overstretching attribution. Nat Clim Change. 2011;1: 2–4. doi:10.1038/nclimate1056

12. Fulton EA. Interesting times: winners, losers, and system shifts under climate change around Australia. ICES J Mar Sci. 2011;68: 1329–1342. doi:10.1093/icesjms/fsr032

13. Allan R, Pereira L, Smith M. Crop evapotranspiration-Guidelines for computing crop water requirements-FAO Irrigation and drainage paper 56. 1998.

14. Hsieh C, Reiss CS, Hewitt RP, Sugihara G. Spatial analysis shows that fishing enhances the climatic sensitivity of marine fishes. Can J Fish Aquat Sci. 2008;65: 947–961. doi:10.1139/f08-017

15. Genner MJ, Sims DW, Southward AJ, Budd GC, Masterson P, Mchugh M, et al. Body size-dependent responses of a marine fish assemblage to climate change and fishing over a century-long scale. Glob Change Biol. 2010;16: 517–527. doi:10.1111/j.1365-2486.2009.02027.x

16. Perry AL, Low PJ, Ellis JR, Reynolds JD. Climate Change and Distribution Shifts in Marine Fishes. Science. 2005;308: 1912–1915. doi:10.1126/science.1111322

17. Pozdnyakov DV, Johannessen OM, Korosov AA, Pettersson LH, Grassl H, Miles MW. Satellite evidence of ecosystem changes in the White Sea: A semi-enclosed arctic marginal shelf sea: WHITE SEA ECOSYSTEM CHANGES. Geophys Res Lett. 2007;34. doi:10.1029/2006GL028947

18. Coll M, Santojanni A, Palomera I, Arneri E. Food-web changes in the Adriatic Sea over the last three decades. Mar Ecol Prog Ser. 2009;381: 17–37. doi:10.3354/meps07944

19. Grbec B, Morović M, Matić F, Marasović I, Vidjak O, Bojanić N, et al. Climate regime shifts and multi-decadal variability of the Adriatic Sea pelagic ecosystem. 2015; 21.

20. Grilli F, Accoroni S, Acri F, Bernardi Aubry F, Bergami C, Cabrini M, et al. Seasonal and Interannual Trends of Oceanographic Parameters over 40 Years in the Northern Adriatic Sea in Relation to Nutrient Loadings Using the EMODnet Chemistry Data Portal. Water. 2020;12: 2280. doi:10.3390/w12082280

21. Bonacci O, Bonacci D, Patekar M, Pola M. Increasing Trends in Air and Sea Surface Temperature in the Central Adriatic Sea (Croatia). J Mar Sci Eng. 2021;9: 358. doi:10.3390/jmse9040358

22. Orel G. Stati di anossia dei fondali, popolamenti bentonici e pesca. Nova Thalass. 1986;8: 267–280.

23. Dulčić, Grbec. Climate change and Adriatic ichthyofauna: Climate change and Adriatic ichthyofauna. Fish Oceanogr. 2000;9: 187–191. doi:10.1046/j.1365-2419.2000.00128.x

24. Bombace G, Lucchetti A. Elementi di biologia della pesca. Milano: Edagricole; 2011.

25. Greenstreet SPR, Hall SJ. Fishing and the Ground-Fish Assemblage Structure in the North-Western North Sea: An Analysis of Long-Term and Spatial Trends. J Anim Ecol. 1996;65: 577. doi:10.2307/5738

26. Papaconstantinou C. The distribution of *Merlangius merlangus euxinus* in the Aegean Sea. Proc 3rd Eur Ichthyol Congr Wars. 1982.

27. Samsun O, Akyol O. Exploitation Rate of Whiting, *Merlangius merlangus* (Linnaeus, 1758) in the Central Black Sea, Turkey. Turk J Marit Mar Sci. 2017;3: 20–26.

28. Keskin Ç. A review of fish fauna in the Turkish Black Sea Karadeniz balık faunası. 2010; 195–207.

29. Jardas I. Jadranska ihtiofauna. Zagreb: Školska knjiga; 1996.

30. Frattini C, Casali P. Distribuzione di Gadiformi in Alto e Medio Adriatico. Biol Mar Medit. 1998;5: 92–98.

31. Atkinson CJL, Bergmann M, Kaiser MJ. Habitat selection in whiting. J Fish Biol. 2004;64: 788–793. doi:10.1111/j.1095-8649.2004.00340.x

32. Piccinetti C, Institut za Oceanografiju i Ribarstvo, editors. Recent state of demersal resources in the Adriatic Sea. Split: Inst. za Oceanografiju i Ribarstvo [u.a.]; 2012.

33. Giovanardi O, Rizzoli M. Biological data, collected during the Pipeta expeditions, on the whiting, *Merlangius merlangus* (L.) in the Adriatic Sea. FAO Fish Rep. 1984.

34. FOOD AND AGRICULTURE ORGANIZATION OF THE UNITED NATIONS. State of mediterranean and black sea fisheries 2018. Place of publication not identified: FOOD & AGRICULTURE ORG; 2019.

35. General Fisheries Commission for the Mediterranean. Resolution GFCM/33/2009/2on the establishment of geographical subareas in the GFCM area of application, amending Resolution GFCM/31/2007/2. 2009.

36. Colantoni P. Aspetti geologici e sedimentologici dell'Adriatico. Atti del convegno nazionale. Ancona; 1985. pp. 17–21.

37. Hopkins TS. The structure of Ionian and Levantine Seas. Rep Meteorol Oceanogr. 1992;41: 35–56.

38. Cozzi S, Giani M. River water and nutrient discharges in the Northern Adriatic Sea: Current importance and long term changes. Cont Shelf Res. 2011;31: 1881–1893. doi:10.1016/j.csr.2011.08.010

39. Campanelli A, Grilli F, Paschini E, Marini M. The influence of an exceptional Po River flood on the physical and chemical oceanographic properties of the Adriatic Sea. Dyn Atmospheres Oceans. 2011;52: 284–297. doi:10.1016/j.dynatmoce.2011.05.004

40. Eigaard OR, Bastardie F, Hintzen NT, Buhl-Mortensen L, Buhl-Mortensen P, Catarino R, et al. The footprint of bottom trawling in European waters: distribution, intensity, and seabed integrity. Kaiser M, editor. ICES J Mar Sci. 2017;74: 847–865. doi:10.1093/icesjms/fsw194

41. Artegiani A, Bregant D, Paschini E, Pinardi N, Raicich F, Russo A. The Adriatic Sea General Circulation. Part I: Air–Sea Interactions and Water Mass Structure. J Phys Oceanogr. 1997;27: 24.

42. Russo A, Carniel S, Sclavo M, Krzelj M. Climatology of the Northern-Central Adriatic Sea. In: Wang S-YS, editor. Modern Climatology. InTech; 2012. doi:10.5772/34693

43. Dorgham MM. Effects of Eutrophication. In: Ansari AA, Gill SS, editors. Eutrophication: Causes, Consequences and Control. Dordrecht: Springer Netherlands; 2014. pp. 29–44. doi:10.1007/978-94-007-7814-6_3

44. Bertrand JA, Gil de Sola L, Papaconstantinou C, Relini G, Souplet A. The general specifications of the MEDITS surveys. Sci Mar. 2002;66: 9. doi:10.3989/scimar.2002.66s29

45. Spedicato MT, Massutí E, Mérigot B, Tserpes G, Jadaud A, Relini G. The MEDITS trawl survey specifications in an ecosystem approach to fishery management. Sci Mar. 2020;83: 9. doi:10.3989/scimar.04915.11X

46. Anonymous. Medits Handbook version 9. Available: http://www.sibm.it/MEDITS%202011/principaledownload.htm

47. Marshall S, Elliott M. Environmental Influences on the Fish Assemblage of the Humber Estuary, U.K. Estuar Coast Shelf Sci. 1998;46: 175–184. doi:10.1006/ecss.1997.0268

48. Teruzzi A, Feudale L, Bolzon G, Lazzari P, Salon S, Di Biagio V, et al. Mediterranean Sea Biogeochemical Reanalysis (CMEMS MED-Biogeochemistry, MedBFM3 system): MEDSEA_MULTIYEAR_BGC_006_008. Copernicus Monitoring Environment Marine Service (CMEMS); 2021. doi:10.25423/CMCC/MEDSEA_MULTIYEAR_BGC_006_008_MEDBFM3

49. Escudier R, Clementi E, Omar M, Cipollone A, Pistoia J, Aydogdu A, et al. Mediterranean Sea Physical Reanalysis (CMEMS MED-Currents, E3R1 system): MEDSEA_MULTIYEAR_PHY_006_004. Copernicus Monitoring Environment Marine Service (CMEMS); 2020. doi:10.25423/CMCC/MEDSEA_MULTIYEAR_PHY_006_004_E3R1

50. Anderson SC, Ward EJ, English PA, Barnett LAK. sdmTMB: an R package for fast, flexible, and user-friendly generalized linear mixed effects models with spatial and spatiotemporal random fields. bioRxiv. 2022; 2022.03.24.485545. doi:10.1101/2022.03.24.485545

51. RStudio Team. RStudio: Integrated Development for R. RStudio, PBC, Boston, MA. 2020. Available: http://www.rstudio.com/

52. Anderson SC, Keppel EA, Edwards AM. A reproducible data synopsis for over 100 species of British Columbia groundfsh. : 328.

53. Essington TE, Anderson SC, Barnett LAK, Berger HM, Siedlecki SA, Ward EJ. Advancing statistical models to reveal the effect of dissolved oxygen on the spatial distribution of marine taxa using thresholds and a physiologically based index. Ecography. 2022;2022. doi:10.1111/ecog.06249

54. Thorson J. Spatio-temporal variation in fish condition is not consistently explained by density, temperature, or season for California Current groundfishes. Mar Ecol Prog Ser. 2015;526: 101–112. doi:10.3354/meps11204

55. Akaike H. Information theory and an extension of the maximum likelihood principle. Second International Symposium on Information Theory. Akademiai Kiado: Budapest, Hungary: Petrov, B.N., Csaki, F; 1973. pp. 267–281.

56. Loots C, Vaz S, Planque B, Koubbi P. Understanding what controls the spawning distribution of North Sea whiting (*Merlangius merlangus*) using a multi-model approach: Spatial distribution of whiting population. Fish Oceanogr. 2011;20: 18–31. doi:10.1111/j.1365-2419.2010.00564.x

57. González-Irusta JM, Wright PJ. Spawning grounds of whiting (*Merlangius merlangus*). Fish Res. 2017;195: 141–151. doi:10.1016/j.fishres.2017.07.005

58. Milić D, Kraljević M. Biometry analysis of the whiting, *Merlangius merlangus* (Linneaus, 1758) from the northern Adriatic Sea. 2010; 13.

59. Bastrikin DK, Gallego A, Millar CP, Priede IG, Jones EG. Settlement length and temporal settlement patterns of juvenile cod (*Gadus morhua*), haddock (*Melanogrammus aeglefinus*), and whiting (*Merlangius merlangus*) in a northern North Sea coastal nursery area. ICES J Mar Sci. 2014;71: 2101–2113. doi:10.1093/icesjms/fsu029

60. Mazlum RE, Bilgin S. Age, growth, reproduction and diet of the whiting, *Merlangius merlangus euxinus* (Nordmann, 1840), in the southeastern Black Sea. Cah Biol Mar. 2014;55: 463–474.

61. Katsanevakis S, Maravelias CD. Bathymetric distribution of demersal fish in the Aegean and Ionian Seas based on generalized additive modeling. Fish Sci. 2009;75: 13–23. doi:10.1007/s12562-008-0033-5

62. Svetovidov AN. Gadiformes (Treskoobraznye). Translated from Russian [by Walter J. Walters with Vladimir Walters]. Jerusalem : Israel Program for Scientific Translations,; 1962. doi:10.5962/bhl.title.46332

63. General Fisheries Commission for the Mediterranean. Report of the seventh meeting of the Subregional Group on Stock Assessment in the Black Sea (SGSABS). 2021. Available: https://www.fao.org/gfcm/technical-meetings/detail/en/c/1442355/

64. Kaschner K, Kesner-Reyes K, Garilao C, Rius-Barile J, Rees T, Froese R. Kaschner, K., K. Kesner-Reyes, C. Garilao, J. Rius-Barile, T. Rees and R. Froese, 2016. AquaMaps: predicted range maps for aquatic species. World wide web electronic publication, www.aquamaps.org, Version 08/2016. [cited 7 Apr 2022]. Available: https://www.fishbase.se/references/FBRefSummary.php?ID=115969

65. Froese R, Pauly D. Search FishBase. [cited 7 Apr 2022]. Available: https://www.fishbase.se/search.php

66. Renaud ML. Hypoxia in Louisiana coastal waters during 1983: Implications for fisheries. The Service; 1986.

67. Vaquer-Sunyer R, Duarte CM. Thresholds of hypoxia for marine biodiversity. Proc Natl Acad Sci. 2008;105: 15452–15457. doi:10.1073/pnas.0803833105

68. Hrycik AR, Almeida LZ, Höök TO. Sub-lethal effects on fish provide insight into a biologically-relevant threshold of hypoxia. Oikos. 2017;126: 307–317. doi:10.1111/oik.03678

69. Tobin D, Wright PJ, Gibb FM, Gibb IM. The importance of life stage to population connectivity in whiting (*Merlangius merlangus*) from the northern European shelf. Mar Biol. 2010;157: 1063–1073. doi:10.1007/s00227-009-1387-7

70. Elliott SAM, Sabatino AD, Heath MR, Turrell WR, Bailey DM. Landscape effects on demersal fish revealed by field observations and predictive seabed modelling. : 13.

71. Pigorini B. Sources and dispersion of recent sediments of the Adriatic Sea. Mar Geol. 1968;6: 187–229. doi:10.1016/0025-3227(68)90031-5

72. Henderson PA. A long-term study of whiting, *Merlangius merlangus* (L) recruitment and population regulation in the Severn Estuary, UK. J Sea Res. 2019;155: 101825. doi:10.1016/j.seares.2019.101825

73. Computer generated distribution maps for *Crangon crangon* (common shrimp). [cited 12 May 2022]. Available: https://www.aquamaps.org/receive.php?type_of_map=regular

74. Computer generated distribution maps for *Sprattus sprattus* (European sprat). [cited 12 May 2022]. Available: https://www.aquamaps.org/receive.php?type_of_map=regular

75. Yildiz T, Karakulak FS. Age, Growth and Mortality of Whiting (*Merlangius merlangus* Linnaeus, 1758) from the Western Black Sea, Turkey. Turk J Fish Aquat Sci. 2019;19. doi:10.4194/1303-2712-v19_9_08

76. Ben Rais Lasram F, Guilhaumon F, Albouy C, Somot S, Thuiller W, Mouillot D. The Mediterranean Sea as a 'cul-de-sac' for endemic fishes facing climate change: A MARINE ENDEMIC HOTSPOT UNDER THREAT. Glob Change Biol. 2010;16: 3233–3245. doi:10.1111/j.1365-2486.2010.02224.x

77. Harley CDG, Randall Hughes A, Hultgren KM, Miner BG, Sorte CJB, Thornber CS, et al. The impacts of climate change in coastal marine systems: Climate change in coastal marine systems. Ecol Lett. 2006;9: 228–241. doi:10.1111/j.1461-0248.2005.00871.x

Supporting information

S1 Fig. Trawl hauls locations per country. The number of hauls conducted per year is reported on the top right of each panel. Missing hauls (e.g., in 2014, 2017, 2019) were conducted in autumn-winter period, thus removed from the analyses to obtain a seasonally homogeneous dataset. In 1999 Croatia did not take part in the data collection.

S2 Fig. Standardized coefficients for the candidate models. The point indicates the mean while the lines represent the 95 % confidence intervals for the fixed effects (a) and the random effects (b). β_{DO} represents the coefficient of the slope related to DO while BP_{DO} represents the estimated breakpoint. σ_{γ} represent the standard deviation of the random year intercept and $\sigma_{\omega}$the standard deviation of the spatial random field.

S3 Fig. Randomized quantile residuals of the best fitting model. Histogram of randomized quantile residuals (a) and residual quantile-quantile plot (b).

S4 Fig. Quantile residuals plotted in space.

S5 Fig. Predicted spatio-temporal changes of whiting biomass density (Kg Km-2). All predictions were made over a 2 km^2 grid.

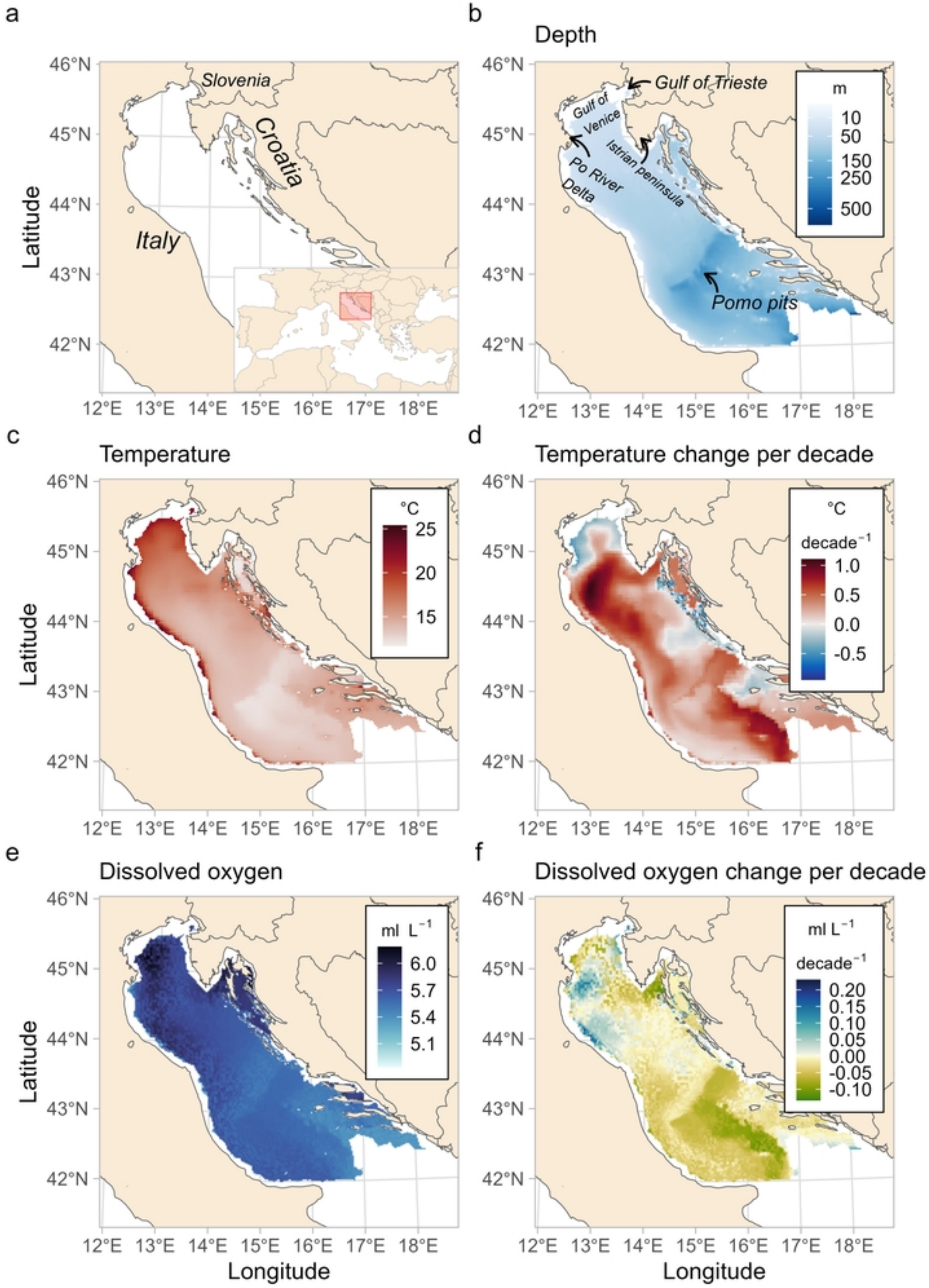
a
Slovenia
Croatia
Italy
Latitude
46°N
45°N
44°N
43°N
42°N
12°E 13°E 14°E 15°E 16°E 17°E 18°E
b
Depth
Gulf of Trieste
Gulf of Venice
Po River Delta
Istrian peninsula
Pomo pits
m
10
50
150
250
500
c
Temperature
°C
25
20
15
d
Temperature change per decade
°C decade⁻¹
1.0
0.5
0.0
-0.5
e
Dissolved oxygen
ml L⁻¹
6.0
5.7
5.4
5.1
f
Dissolved oxygen change per decade
ml L⁻¹ decade⁻¹
0.20
0.15
0.10
0.05
0.00
-0.05
-0.10
Longitude

Figure

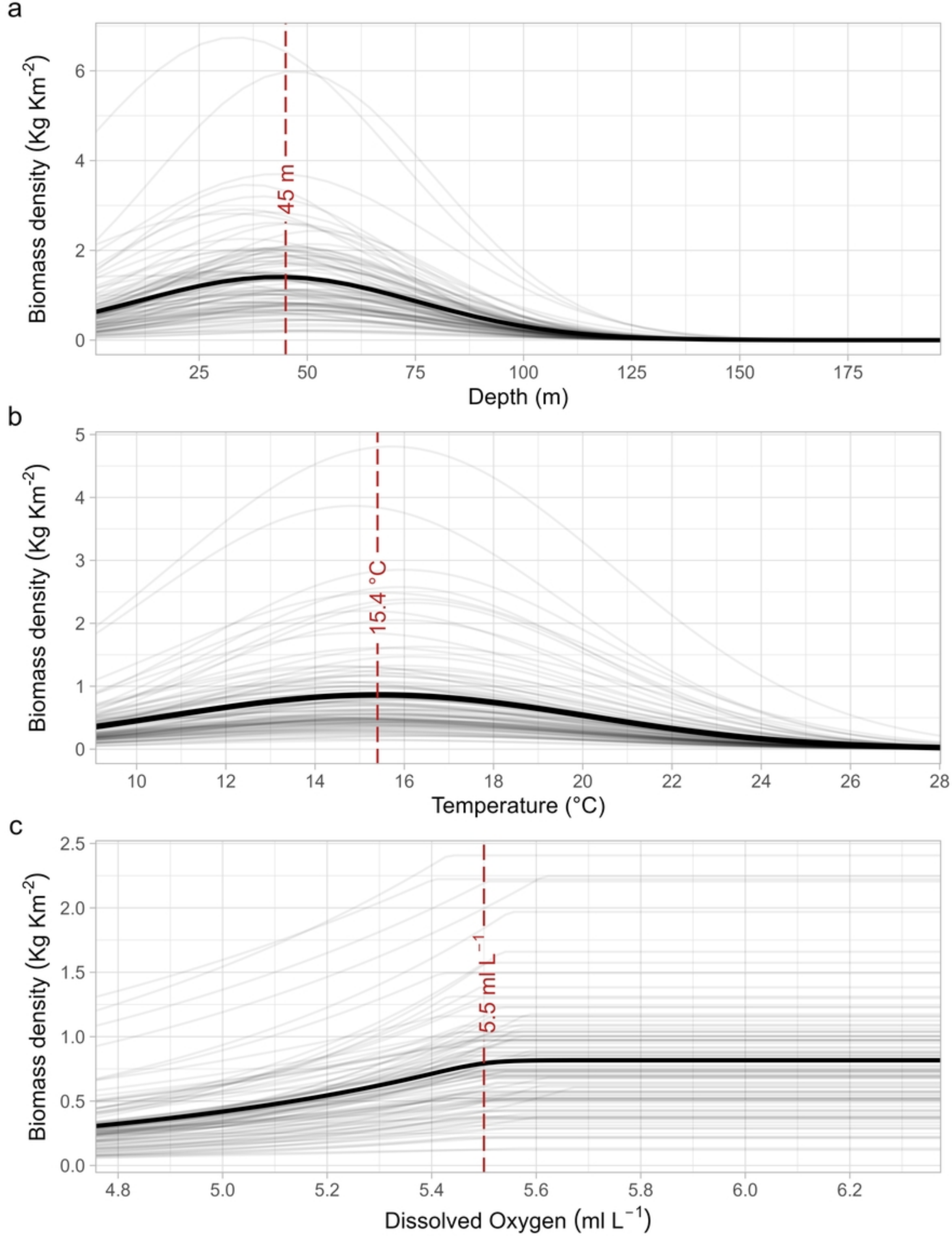
a
Biomass density (Kg Km^{-2})
45 m
Depth (m)
b
Biomass density (Kg Km^{-2})
15.4 °C
Temperature (°C)
c
Biomass density (Kg Km^{-2})
5.5 ml L^{-1}
Dissolved Oxygen (ml L^{-1})

Figure

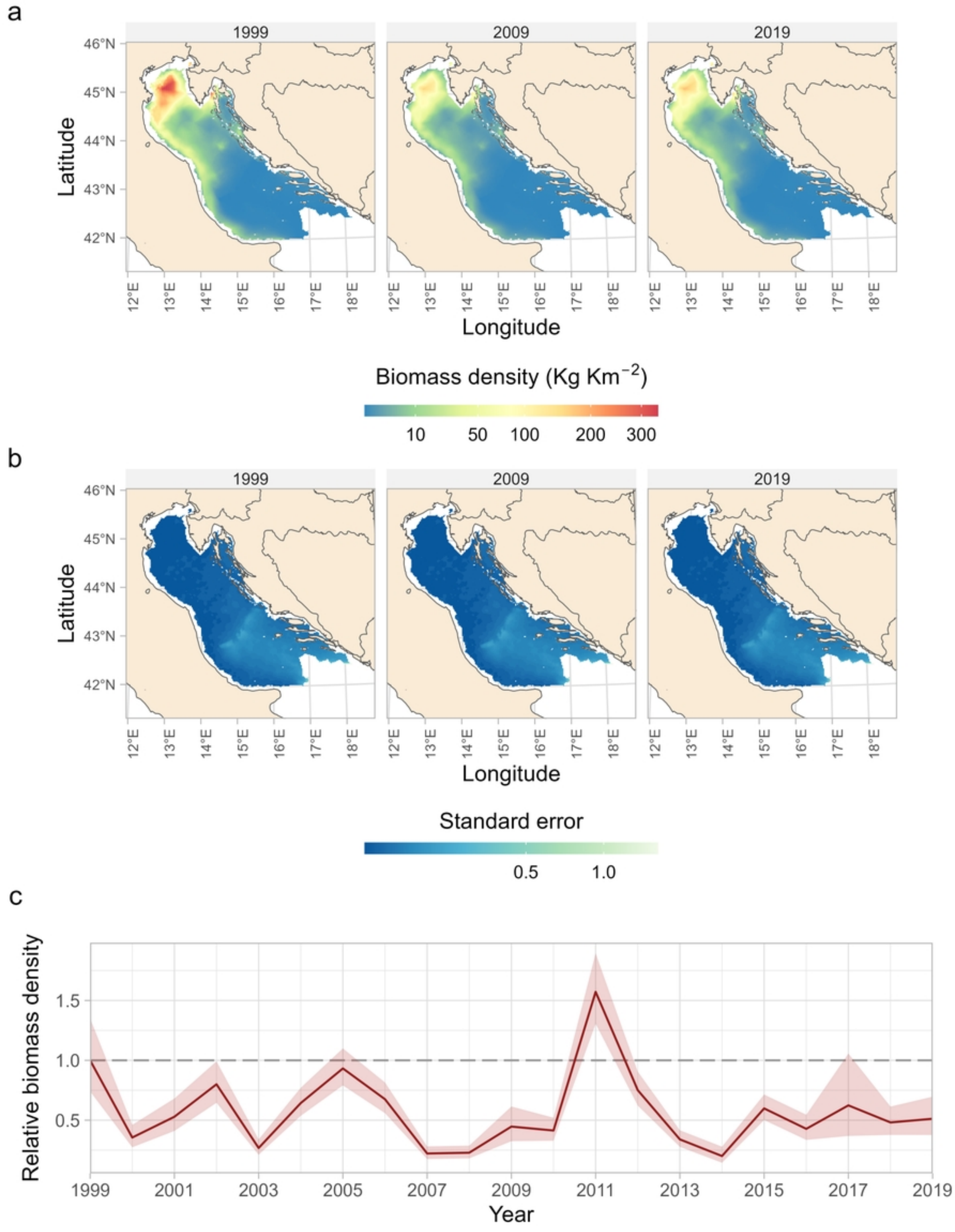
a
1999
2009
2019
46°N
45°N
44°N
43°N
42°N
Latitude
12°E
13°E
14°E
15°E
16°E
17°E
18°E
Longitude
Biomass density (Kg Km^{-2})
10
50
100
200
300
b
1999
2009
2019
46°N
45°N
44°N
43°N
42°N
Latitude
12°E
13°E
14°E
15°E
16°E
17°E
18°E
Longitude
Standard error
0.5
1.0
c
Relative biomass density
1.5
1.0
0.5
1999
2001
2003
2005
2007
2009
2011
2013
2015
2017
2019
Year

Figure

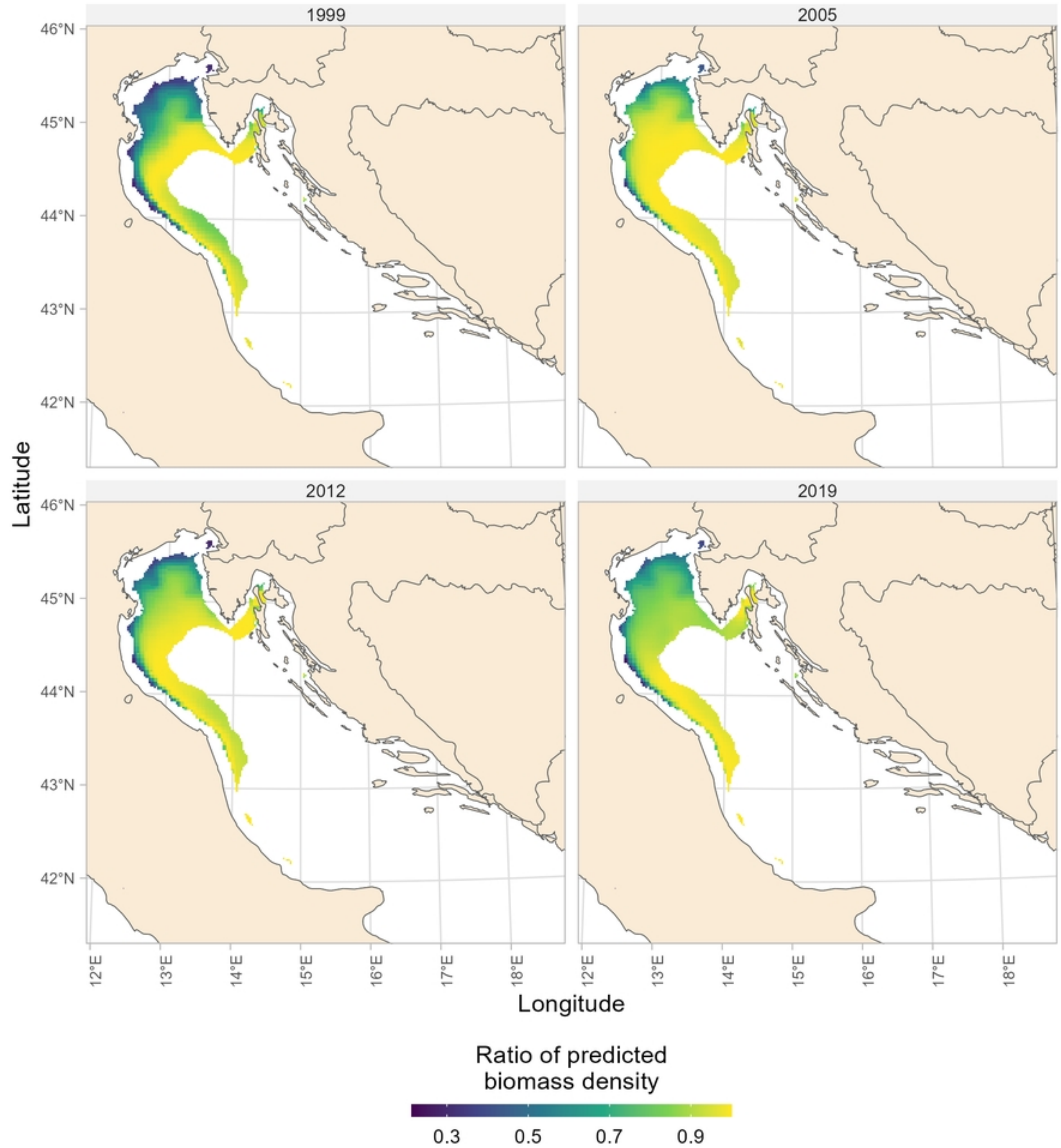
1999
2005
2012
2019
46°N
45°N
44°N
43°N
42°N
Latitude
12°E
13°E
14°E
15°E
16°E
17°E
18°E
Longitude
Ratio of predicted biomass density
0.3
0.5
0.7
0.9

Figure

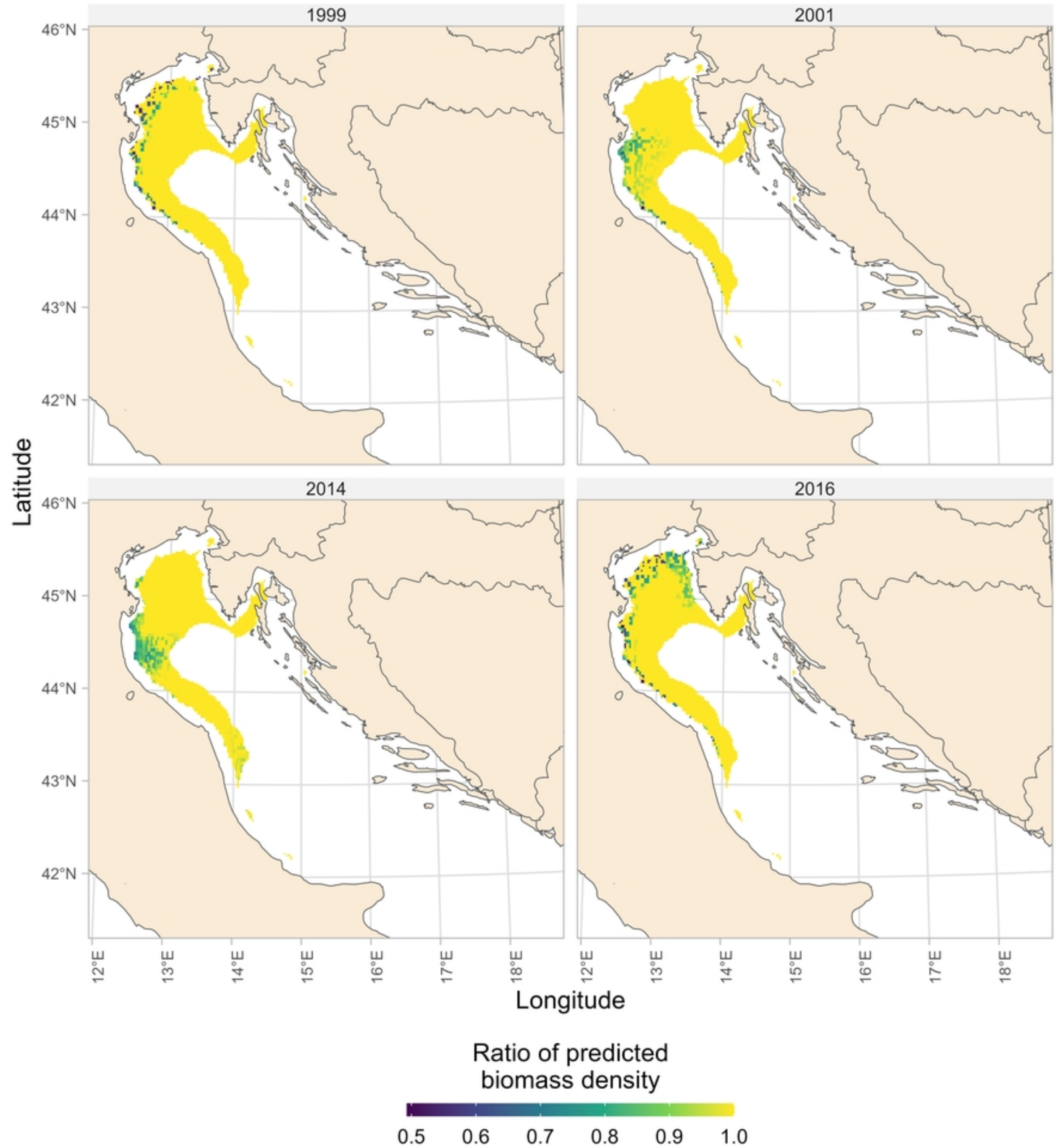
1999
2001
2014
2016
46°N
45°N
44°N
43°N
42°N
Latitude
12°E
13°E
14°E
15°E
16°E
17°E
18°E
Longitude
Ratio of predicted biomass density
0.5
0.6
0.7
0.8
0.9
1.0

Figure